

Real-Time Energy-Optimal Trajectory Generation for a Servo Motor

Zhao, Y.; Wang, Y.; Bortoff, S.A.; Ueda, K.

TR2013-056 June 2013

Abstract

This paper considers the fast generation of speed and acceleration constrained energy-optimal trajectories for a motor system performing a point-to-point positioning task with a fixed final time. An algorithm is proposed to obtain the energy-optimal solution by solving a series of Two-point Boundary Value Problems (TBVPs) with guaranteed convergence. The algorithm is capable of generating energy-optimal trajectories in real-time.

American Control Conference (ACC)

This work may not be copied or reproduced in whole or in part for any commercial purpose. Permission to copy in whole or in part without payment of fee is granted for nonprofit educational and research purposes provided that all such whole or partial copies include the following: a notice that such copying is by permission of Mitsubishi Electric Research Laboratories, Inc.; an acknowledgment of the authors and individual contributions to the work; and all applicable portions of the copyright notice. Copying, reproduction, or republishing for any other purpose shall require a license with payment of fee to Mitsubishi Electric Research Laboratories, Inc. All rights reserved.

Real-Time Energy-Optimal Trajectory Generation for a Servo Motor

Yiming Zhao, Yebin Wang, Scott A. Bortoff, and Koichiro Ueda

Abstract—This paper considers the fast generation of speed and acceleration constrained energy-optimal trajectories for a motor system performing a point-to-point positioning task with a fixed final time. An algorithm is proposed to obtain the energy-optimal solution by solving a series of Two-point Boundary Value Problems (TBVPs) with guaranteed convergence. The algorithm is capable of generating energy-optimal trajectories in real-time.

Index Terms—servo motor, motion control, trajectory generation, minimum energy, optimal control, boundary value problem, real-time, speed constraint, acceleration constraint.

I. INTRODUCTION

In a motor position control task, which is essential to numerous mechatronic systems, the motor transits from one angular position to another in a certain amount of time with zero initial and final speed. Time-optimal and approximate time-optimal motor trajectory generation problems have been considered for servo position control and motor speed response control [11], [9], [2], [8], [13], [7], [1], [3]. To improve the unsatisfactory energy efficiency of time-optimal motor positioning trajectories, the energy-optimal motor position control problem has also been studied. Ref. [12] proposed an energy-optimal control method for incremental motion drive (IMD), which used the optimal control technique to compute the current control inputs and execution time to minimize the resistive loss of the motor. This method does not take into account the friction of the system. Neither does it consider the mechanical power stored in the rotor and load which can help with the positioning task. Reference [10] revised this method to consider friction and mechanical power, and seeks for a suboptimal solution by introducing a power cut-off disconnection time splitting the overall motion into two phases. Ref. [6] studied the problem of energy-optimal translation for a two wheeled robot, which is equivalent to a motor position control problem, and proposed a real-time algorithm based on optimal control. However, similar to previous research in [12], [10], it does not consider speed and acceleration constraints, which are important for addressing actuator limitations, vibration attenuation, and safety.

A trapezoidal speed profile has been used for the energy efficient control of a permanent magnet synchronous

motor (PMSM) [4], and the energy-saving speed control of a wheeled mobile robot [5]. Although this method can consider both acceleration and speed constraints, the result is obviously suboptimal. It is expected that more energy saving can be achieved using the optimal control approach.

The main contribution of this paper is twofold. First, the energy-optimal servo motor position control problem is studied using an optimal control formulation including both acceleration and speed constraints, which has not been addressed in the previous research using optimal control. Second, this paper proposes a novel computationally efficient algorithm which solves the acceleration and speed constrained energy-optimal trajectory generation problem with guaranteed convergence.

This paper is organized as follows: The problem statement is provided in Section II. Section III presents the theoretical results and the algorithms for computing energy-optimal motor position control trajectories. The validity and efficiency of the proposed algorithm are demonstrated by numerical simulation in Section IV.

II. PROBLEM STATEMENT

Let x be the angular position of the motor, $v = \dot{x}$ be the angular speed, and u be the control current. The speed dynamics equation of the motor system is given by

$$I\dot{v}(t) = -d_0v(t) - c_0 + K_t u(t),$$

where I is the combined moment of inertia of the motor and the load, c_0 is the Coulomb friction constant, d_0 is the viscous friction coefficient, and K_t is the torque constant. Since the motor speed is either positive or negative along an energy-optimal positioning trajectory except at t_0 and t_f , it is justified to treat the Coulomb friction as constant as in the above dynamics equation. For notational convenience, let $d = d_0/I$, $c = c_0/I$ and $b = K_t/I$, the motor system dynamics can be written as

$$\dot{x}(t) = v(t), \quad (1)$$

$$\dot{v}(t) = -dv(t) - c + bu(t), \quad (2)$$

In order to reduce structure vibration and maintain motor efficiency, it is required that the motor's motion must satisfy the speed and acceleration constraints:

$$v(t) \leq v_{\max}, \quad (3)$$

$$A_{\min} \leq \dot{v} = -dv(t) - c + bu(t) \leq A_{\max}, \quad (4)$$

where v_{\max} , A_{\min} , and A_{\max} are constants with $A_{\min} < 0$ and $A_{\max} > 0$. As in [6], we model the energy consumption of motor as a sum of copper loss and mechanical work. A

Y. Zhao, Y. Wang, and S. A. Bortoff are with Mitsubishi Electric Research Laboratories, 201 Broadway, Cambridge, MA, 02139, USA. Phone: +1617621-7500, fax: +1617621-7550, {yzhao, yebinwang, bortoff}@merl.com

K. Ueda is with the Advanced Technology R&D Center, Mitsubishi Electric Corporation, 8-1-1, Tsukaguchi-honmachi, Amagasaki City, 661-8661, Japan. Ueda.Koichiro@da.MitsubishiElectric.co.jp

formula for the instantaneous power of the motor is given by

$$P(v, u) = Ru^2 + K_t v u, \quad (5)$$

where R is the resistance of the motor. The energy-optimal trajectory is given by the solution to the following minimum energy control problem:

Problem 1 (Energy-optimal motor position control):

$$\begin{aligned} \min_u \quad & E = \int_0^{t_f} P(v(t), u(t)) dt \\ \text{s.t.} \quad & \dot{x}(t) = v(t), \\ & \dot{v}(t) = -dv(t) - c + bu(t), \\ & v(t) \leq v_{\max}, \\ & A_{\min} \leq -dv(t) - c + bu(t) \leq A_{\max}, \\ & x(0) = 0, x(t_f) = x_f, \\ & v(0) = 0, v(t_f) = 0. \end{aligned}$$

Without loss of generality, we assume $x_f > 0$. Note that the speed regulation problem is just a simplified version of Problem 1, therefore the method proposed later in this paper also applies to energy-optimal motor speed response control.

III. OPTIMAL SOLUTION AND ALGORITHMS

We propose a computationally efficient method for solving Problem 1 using optimal control theory. The key idea is the application of an analytic solution to the Two-point Boundary Value Problem (TBVP) associated with Problem 1 when the constraints (3) and (4) are inactive, which is referred to as the unconstrained case henceforth. Based on the analytic solution, a novel algorithm is designed for updating the boundary conditions of a series of TBVPs such that the TBVP solutions converge to that of Problem 1. The schema of the proposed method is illustrated in Fig. 1, where ‘BC’ stands for boundary condition.

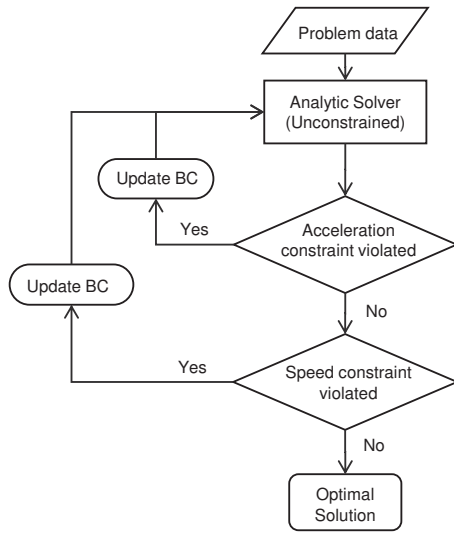


Fig. 1. Schematic for minimum energy servo control.

A. Analytic Solution of the Unconstrained Case

In this section we present the analytic solution to problem 1 for the unconstrained case, which is reformulated below:

Problem 2: (Unconstrained energy-optimal motor position control problem)

$$\begin{aligned} \min_u \quad & E = \int_0^{t_f} (Ru^2(t) + K_t v(t)u(t)) dt \\ \text{s.t.} \quad & \dot{x}(t) = v(t), \\ & \dot{v}(t) = -dv(t) - c + bu(t), \\ & x(0) = 0, x(t_f) = x_f, \\ & v(0) = 0, v(t_f) = 0. \end{aligned}$$

Problem 2 can be solved analytically by applying Pontryagin's Maximum Principal. The Hamiltonian for this problem is

$$\begin{aligned} H(x(t), v(t), \lambda_x(t), \lambda_v(t), u(t)) \\ = Ru^2(t) + K_t v(t)u(t) + \lambda_x(t)v(t) \\ + \lambda_v(t)(-dv(t) - c + bu(t)), \end{aligned}$$

where λ_x and λ_v are the co-state variables. The dynamics of the co-states are given by

$$\dot{\lambda}_x(t) = -\frac{\partial H}{\partial x} = 0, \quad (6)$$

$$\dot{\lambda}_v(t) = -\frac{\partial H}{\partial v} = d\lambda_v(t) - K_t u(t) - \lambda_x(t). \quad (7)$$

According to (6), $\lambda_x(t)$ is constant. The optimal control u^* can be determined from the first-order optimality condition $\partial H / \partial u = 0$, which yields

$$u^*(t) = -\frac{K_t}{2R}v(t) - \frac{b}{2R}\lambda_v(t). \quad (8)$$

It is also noted that

$$\frac{\partial^2 H}{\partial u^2} = 2R > 0, \quad (9)$$

which ensures that u^* is unique.

Substituting (8) into the state and co-state dynamics, we have the following linear TBVP

$$\dot{x}(t) = v(t), \quad (10)$$

$$\dot{v}(t) = -\left(d + \frac{bK_t}{2R}\right)v(t) - \frac{b^2}{2R}\lambda_v(t) - c, \quad (11)$$

$$\dot{\lambda}_v(t) = \frac{K_t^2}{2R}v(t) + \left(d + \frac{bK_t}{2R}\right)\lambda_v(t) - \lambda_x, \quad (12)$$

with boundary conditions $x(0) = 0, x(t_f) = x_f, v(0) = 0, v(t_f) = 0$, and unknown parameter $\lambda_x, \lambda_v(0)$ and $\lambda_v(t_f)$. Let $A_1 = -(d + \frac{bK_t}{2R}), A_2 = -\frac{b^2}{2R}, A_3 = \frac{K_t^2}{2R}$, and define

$$A = \begin{bmatrix} 0 & 1 & 0 \\ 0 & A_1 & A_2 \\ 0 & A_3 & -A_1 \end{bmatrix}, \quad B = \begin{bmatrix} 0 \\ -c \\ -\lambda_x \end{bmatrix}.$$

Differential equations in the above TBVP can be written as

$$\dot{X}(t) = AX(t) + B \quad (13)$$

where $X(t) = [x(t), v(t), \lambda_v(t)]^T$. The analytic solution to (13) is given by

$$X(t) = M(t, t_0)X(t_0) + G(t, t_0)B, \quad (14)$$

where $M(t, t_0) = e^{A(t-t_0)} \in \mathbb{R}^{3 \times 3}$ is the state-transition matrix. The matrix $G(t, t_0) \in \mathbb{R}^{3 \times 3}$ is given by

$$G(t, t_0) = \int_{t_0}^t e^{A(t-\tau)} d\tau.$$

Both $M(t, t_0)$ and $G(t, t_0)$ can be easily computed analytically using standard symbolic computation software, hence are not listed here due to limited space. The boundary conditions of the TBVP must satisfy (14) with $t = t_f$ as described by the following linear algebraic equations,

$$X(t_f) = M(t_f, 0)X(t_0) + G(t_f, 0)B, \quad (15)$$

from which the three unknowns $\lambda_{v_0} = \lambda_v(0)$, $\lambda_{v_f} = \lambda_v(t_f)$, and λ_x can be easily solved. Once these unknowns are obtained, the optimal state and co-state trajectories as the solution to the TBVP (13) can be determined from (14), and the corresponding optimal control is given by (8).

The following two propositions characterize some properties of the energy-optimal speed profile in the unconstrained case, which will be used later. The proof of Proposition 1 is omitted due to space limitation.

Proposition 1: Let $(x, v, \lambda_x, \lambda_v)$ and $(\tilde{x}, \tilde{v}, \tilde{\lambda}_x, \tilde{\lambda}_v)$ be two sets of optimal states and co-states for Problem 2 with different boundary conditions and/or final time t_f such that v and \tilde{v} are not identical, then the function $z(t) = v(t) - \tilde{v}(t)$ has at most two roots. Furthermore, suppose the function z has at least one root, then its derivative $\dot{z}(t) = \dot{v}(t) - \dot{\tilde{v}}(t)$ has at most one root.

Proposition 2: Let $(x, v, \lambda_x, \lambda_v)$ be the optimal solution for Problem 2. Suppose there exists $t_1, t_2 \in \mathbb{R}$ such that $\dot{v}(t_1)\dot{v}(t_2) < 0$, then $\dot{v}(t)$ is a strictly monotone function.

Proof: Based on the analytic solution to Problem 2, it can be shown that

$$\begin{aligned} \dot{v}(t) = & (A_2\lambda_{v_0} - c + A_1v_0) \cosh(pt/2) \\ & + 2(v_0A_1^2 - cA_1 - A_2\lambda_x + A_2A_3v_0) \sinh(pt/2)/p. \end{aligned}$$

Let $\tau = pt/2$. Noticing that $\sinh(\tau) = (e^\tau - e^{-\tau})/2$ and $\cosh(\tau) = (e^\tau + e^{-\tau})/2$, there exist constants $c_1, c_2 \in \mathbb{R}$ such that the above expression can be rewritten as

$$v'(\tau) = c_1e^\tau + c_2e^{-\tau},$$

where v' denotes the derivative of v with respect to τ . Besides, with $\tau_1 = pt_1/2$ and $\tau_2 = pt_2/2$, we have $v'(\tau_1)v'(\tau_2) < 0$. Without loss of generality, assume that $\tau_1 < \tau_2$. Since v' is proportional to \dot{v} , it suffices to prove that v' is a strictly monotone function.

If $v'(\tau_1) > 0$ and $v'(\tau_2) < 0$, then we must have $c_1c_2 < 0$, otherwise, $v'(\tau)$ is either always positive or always negative, which leads to a contradiction. Now consider the second derivative of v :

$$v''(\tau) = c_1e^\tau - c_2e^{-\tau}.$$

Note that $v''(\tau)$ is a continuous function. Because $c_1c_2 < 0$, we must have either $v''(\tau) > 0$ for any $\tau \in \mathbb{R}$ when $c_1 > 0$, or that $v''(\tau) < 0$ for any $\tau \in \mathbb{R}$ when $c_1 < 0$, which implies that $v'(\tau) > 0$ is either a strictly monotone increasing function when $c_1 > 0$ or a strictly monotone decreasing function when $c_1 < 0$. Similar conclusion holds when $v'(\tau_1) < 0$ and $v'(\tau_2) > 0$. Therefore, the proof is complete. \blacksquare

B. Trajectory Smoothness at Junction Points

In the sequel, when $v(t) = v_{\max}$ along a segment of the speed profile, this segment is referred to as a speed constrained arc. Similarly, the activation of constraints $\dot{v} \leq A_{\max}$ and $\dot{v} \geq A_{\min}$ corresponds to acceleration constrained and deceleration constrained arcs, respectively. The connection points between neighboring arcs are called *junction points*. For Problem 1, because the Hamiltonian is strictly convex with respect to the control according to (9), and the fact that the constraints are linearly independent, the optimal control is continuous along the whole trajectory, and the slope of the optimal speed profile for Problem 1 is continuous at any time, including the junction points.

C. Energy-Optimal Control with Acceleration Constraints

When the acceleration constraints are active, the optimal solution typically exhibits a three phase structure: acceleration constrained trajectory, unconstrained trajectory, and deceleration constrained trajectory. The optimal solution may not contain the first or the third phase depending on values of A_{\max} and A_{\min} . However, the proposed method can still be applied without any difficulty. Hence, we focus on the general case and assume that the optimal solution contains three phases.

In the first and third phases, the position and speed can be determined by

$$v_l(t) = A_{\max}t, \quad (16)$$

$$x_l(t) = \frac{1}{2}A_{\max}t^2, \quad (17)$$

$$v_r(t) = A_{\min}(t - t_f), \quad (18)$$

$$x_r(t) = x_f + \frac{1}{2}A_{\min}(t - t_f)^2. \quad (19)$$

which satisfy the boundary conditions at t_0 and t_f . Let (x_m, v_m, u_m) be the optimal solution of the second phase on the time interval $[t_1, t_2]$ with boundary values $x_l(t_1)$, $v_l(t_1)$ and $x_r(t_2)$, $v_r(t_2)$, where t_1 is the switch time between the acceleration constrained and unconstrained arcs, t_2 is the switch time between the unconstrained and deceleration constrained arcs, as illustrated in Fig. 2. Since the constraints are inactive in the second phase, the optimal solution during this phase is given by

$$\begin{bmatrix} x_m(t) \\ v_m(t) \\ \lambda_v(t) \end{bmatrix} = M(t, t_1) \begin{bmatrix} x_m(t_1) \\ v_m(t_1) \\ \lambda_v(t_1) \end{bmatrix} - G(t, t_1) \begin{bmatrix} 0 \\ c \\ \lambda_x \end{bmatrix}, \quad (20)$$

The optimal solution x_m and v_m must also satisfy the junction conditions $x_m(t_1) = x_l(t_1)$, $v_m(t_1) = v_l(t_1)$,

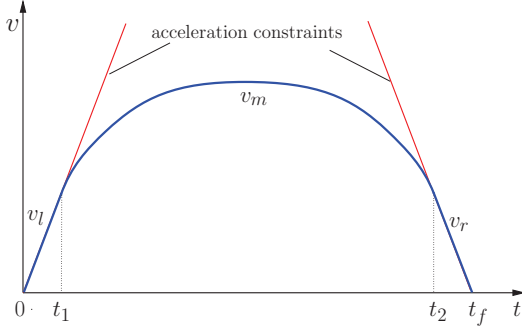


Fig. 2. Optimal speed profile with active acceleration constraints.

$x_m(t_2) = x_r(t_2)$, $v_m(t_2) = v_r(t_2)$. Since the energy-optimal speed profile does not contain any corner point, we have $\dot{v}_l(t_1^-) = \dot{v}_m(t_1^+)$ and $\dot{v}_m(t_2^-) = \dot{v}_r(t_2^+)$.

Algorithm 1 is proposed for solving the acceleration constrained problem by identifying the optimal switch times t_1 , t_2 satisfying all junction conditions. Once t_1 and t_2 are obtained, the optimal trajectory can be easily computed. According to the following theorem, the switching times given by Algorithm 1 always converge to the optimal values.

Theorem 3.1: The sequences $\{t_{a_k}\}$ and $\{t_{b_k}\}$ as updated in Algorithm 1 converge monotonically to the optimal switching times t_1^* and t_2^* , respectively, as $k \rightarrow \infty$.

The proof of Theorem 3.1 is omitted due to space limitation. Figure 3 illustrates one step of updates for switching times using Algorithm 1 when both the acceleration and deceleration constraints are violated.

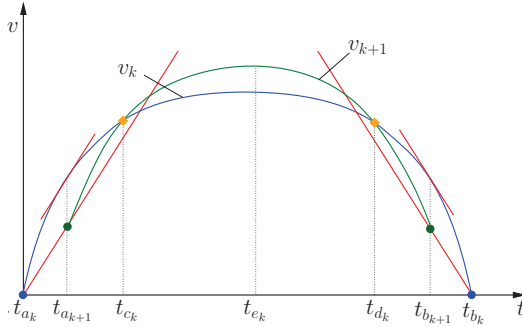


Fig. 3. Update scheme of switching time.

D. Energy-Optimal Control with Acceleration and Speed Constraints

In this section we propose an algorithm dealing with the maximum speed constraint. This algorithm is based on a partial equivalence between the optimal solution to Problem 1 and the optimal solution to a particular problem with acceleration constraint only, which can be solved using Algorithm 1. Such a partial equivalence is illustrated in Fig. 4, and the details are given by Theorem 3.2. Theorem 3.2 is given without proof due to space limitation.

Theorem 3.2: Let (x^*, v^*, u^*) be the optimal solution to Problem 1 with final position x_f and final time t_f . Suppose

Algorithm 1 Switch time computation for active acceleration constraints

- 1: $e \leftarrow 1$, $k \leftarrow 1$, and choose a small tolerance parameter $\varepsilon \ll 1$
- 2: $t_{a_k} \leftarrow 0$, $t_{b_k} \leftarrow t_f$
- 3: **while** $e > \varepsilon$ **do**
- 4: solve the unconstrained problem with boundary conditions $v_k(t_{a_k}) = v_l(t_{a_k})$, $x_k(t_{a_k}) = x_l(t_{a_k})$, $v_k(t_{b_k}) = v_r(t_{b_k})$, $x_k(t_{b_k}) = x_r(t_{b_k})$, and denote the solution as (x_k, v_k, u_k) .
- 5: **if** $\dot{v}_k(t_{a_k}) > A_{\max}$ **then**
- 6: solve $\dot{v}_k(\tau_l) = A_{\max}$ for τ_l
- 7: $t_{a_{k+1}} \leftarrow \tau_l$
- 8: **else**
- 9: $t_{a_{k+1}} \leftarrow t_{a_k}$
- 10: **end if**
- 11: **if** $\dot{v}_k(t_{b_k}) < A_{\min}$ **then**
- 12: solve $\dot{v}_k(\tau_r) = A_{\min}$ for τ_r
- 13: $t_{b_{k+1}} \leftarrow \tau_r$
- 14: **else**
- 15: $t_{b_{k+1}} \leftarrow t_{b_k}$
- 16: **end if**
- 17: $k \leftarrow k + 1$
- 18: $e \leftarrow |t_{a_k} - t_{a_{k-1}}| + |t_{b_k} - t_{b_{k-1}}|$
- 19: **end while**
- 20: $t_1 \leftarrow t_{a_k}$, $t_2 \leftarrow t_{b_k}$
- 21: **return** x^* , v^* , u^* , where

$$x^*(t) = \begin{cases} x_l(t), & 0 \leq t \leq t_1, \\ x_k(t), & t_1 < t \leq t_2, \\ x_r(t), & t_2 < t \leq t_f, \end{cases}$$

$$v^*(t) = \begin{cases} v_l(t), & 0 \leq t \leq t_1, \\ v_k(t), & t_1 < t \leq t_2, \\ v_r(t), & t_2 < t \leq t_f, \end{cases}$$

$$u^*(t) = \begin{cases} (A_{\max} + dv_l(t) + c)/b, & 0 \leq t \leq t_1, \\ u_k(t), & t_1 < t \leq t_2, \\ (A_{\min} + dv_r(t) + c)/b, & t_2 < t \leq t_f, \end{cases}$$

the speed constraint $v \leq v_{\max}$ is active on the interval $[t_3^*, t_4^*]$, where t_3^* and t_4^* are the optimal switch times at which v^* enters and exits the speed constrained arc. Let $\Delta_t^* = t_4^* - t_3^*$, and let $(\tilde{x}^*, \tilde{v}^*, \tilde{u}^*)$ be the optimal solution to Problem 1 without the speed constraint and with the final position $x_f - \Delta_t^* v_{\max}$ and the final time $t_f - \Delta_t^*$, then (x^*, v^*, u^*) and $(\tilde{x}^*, \tilde{v}^*, \tilde{u}^*)$ are related by

$$\begin{cases} x^*(t) = \tilde{x}^*(t) \\ v^*(t) = \tilde{v}^*(t) \\ u^*(t) = \tilde{u}^*(t) \end{cases}, \quad t \in [0, t_3^*], \quad (21)$$

$$\begin{cases} x^*(t) = \tilde{x}^*(t - \Delta_t^*) + \Delta_t^* v_{\max} \\ v^*(t) = \tilde{v}^*(t - \Delta_t^*) \\ u^*(t) = \tilde{u}^*(t - \Delta_t^*) \end{cases}, \quad t \in [t_4^*, t_f]. \quad (22)$$

Lemma 1: Let (x^*, v^*, u^*) be the optimal solution to

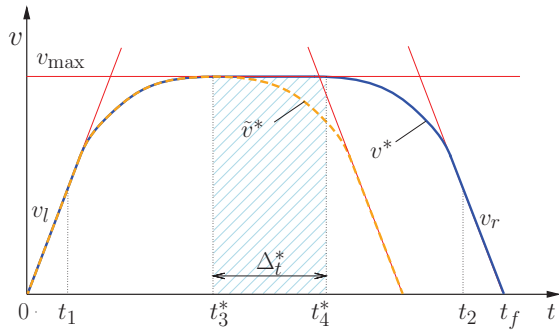


Fig. 4. Optimal speed profile with speed constraint.

Problem 1. Suppose that the state constraint $v - v_{\max} \leq 0$ is activated along v^* . Let $\Gamma \in [0, t_f]$ be the collection of t such that $v^*(t) = v_{\max}$, then Γ is connected.

Lemma 1 means that the optimal speed trajectory to Problem 1 may contain at most one speed constrained arc, which justifies the assumption used in Algorithm 2 that the speed constrained arc is simply connected. Proof of Lemma 1 is omitted due to space limitation.

Algorithm 2 is essentially a bisection algorithm combined with the Newton's update to find the root of the equation $\eta(\delta) = 0$. The Newton's update can help improve the convergence rate when the current update is close to the root of $\eta(\delta) = 0$. It can be shown that $\eta(\delta)$ is continuous and has a unique root on $[0, \Delta_w]$, hence the convergence of Algorithm 2 is guaranteed by the bisection algorithm. The proof for the convergence of Algorithm 2 is omitted due to the page limit. Since Algorithm 1 is used in the inner loop of Algorithm 2, the result of Algorithm 2 satisfies both acceleration/deceleration constraints and speed constraints.

IV. SIMULATION RESULTS

Algorithm 1 and 2 are implemented in Matlab, and executed on a computer with a dual core 2.4GHz CPU. The numerical simulation covers 64 motor position control tasks. In each task, the algorithms determine the structure of the optimal solution, compute the optimal switching times, and return an optimal trajectory. The shortest computation time for a single task is 3.1ms, which corresponds to an unconstrained case. The longest computation time is 33.7 ms for a task involving active acceleration and speed constraints. The average computation time is 6.9 ms. As a comparison, a Nonlinear Programming based numerical optimal control algorithm via direct transcription need 2.5-4.8 s to solve a single task with acceptable accuracy.

Figures 5 and 6 show the optimal speed and control of four position control tasks with the same final position x_f but different final time $t_f = T_0(1 + \alpha)$ for different α values, where T_0 is the minimum time for the positioning task from 0 to x_f , and α is a parameter used for relaxing the final time. The minimum time solution corresponds to the trajectories with $\alpha = 0$ in Figs. 5 and 6. When $\alpha = 0.05$, the optimal speed history contains five phases: acceleration constrained arc, unconstrained arc, speed constrained arc, a second

unconstrained arc, and deceleration constrained arc. When α increases, the maximum speed of the motor decreases, as shown in Fig. 5, which helps with energy saving. When $\alpha = 0.1$, the optimal speed profile contain three phases with active acceleration constraints. The trajectory become unconstrained when $\alpha = 0.5$. It is clear from these figures that the acceleration and speed constraints are satisfied by the algorithm's solutions.

Figure. 7 illustrates the trade-off between energy consumption and transition time for the same tasks in Fig. 5 and Fig. 6, where α is the parameter for final time relaxation. The energy consumption ratio is the ratio of the energy consumption $E(\alpha)$ of the minimum energy trajectory by Algorithm 2 to the energy cost $E_t(\alpha)$ of the trapezoidal speed profile introduced in Ref. [4]. When $\alpha = 0$, the trapezoidal speed profile becomes the minimum-time solution. It is obvious from Fig. 7 that considerable energy saving (up to more than 40%) can be achieved by relaxing the transition time and applying the minimum energy servo control.

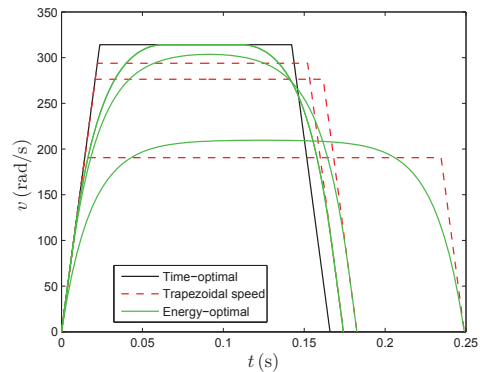


Fig. 5. Optimal speed profile.

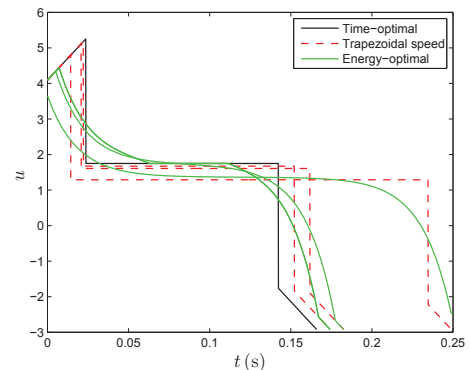


Fig. 6. Optimal control profile.

V. CONCLUSIONS

The proposed energy-optimal trajectory generation method solves the acceleration and speed constrained energy-optimal control problem for a servomotor system on the scale of a

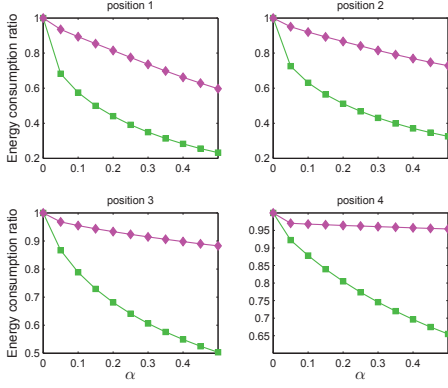


Fig. 7. Energy consumption ratios versus α . The green square markers are $E(\alpha)/E_t(0)$, and the magenta diamond markers are $E(\alpha)/E_t(\alpha)$ for different α values.

few milliseconds. The corresponding algorithm is guaranteed to converge to the optimal solution. The proposed method is suitable for real-time applications.

REFERENCES

- [1] M. I. Bayindir, H. Can, Z. H. Akpolat, M. Ozdemir, and E. Akin, "Robust quasi-time-optimal discrete-time sliding mode control of a servomechanism," *Electric Power Components and Systems*, vol. 35, no. 8, pp. 885–905, 2007.
- [2] K.-T. Chang, T.-S. Low, and T.-H. Lee, "An optimal speed controller for permanent-magnet synchronous motor drives," *IEEE Transactions on Industrial Electronics*, vol. 41, no. 5, pp. 503–510, Oct. 1994.
- [3] Y.-M. Choi, J. Jeong, and D.-G. Gweon, "Modified damping scheduling proximate time optimal servomechanism for improvements in short strokes in hard disk drives," *IEEE Transactions on Magnetics*, vol. 44, no. 4, pp. 540–546, Apr. 2008.
- [4] S. Dodds, "Sliding mode vector control of pmsm drives with minimum energy position following," in *Proceedings of the 13th Power Electronics and Motion Control Conference*, Sep. 2008, pp. 2559–2566.
- [5] C. H. Kim and B. K. Kim, "Energy-saving 3-step velocity control algorithm for battery-powered wheeled mobile robots," in *Proceedings of the IEEE International Conference on Robotics and Automation*, Apr. 2005, pp. 2375–2380.
- [6] —, "Minimum-energy translational trajectory generation for differential-driven wheeled mobile robots," *Journal of Intelligent & Robotic Systems*, vol. 49, no. 4, pp. 367–383, 2007.
- [7] C. La-orphacharapan and L. Y. Pao, "Shaped time-optimal feedback control for disk-drive systems with back-electromotive force," *IEEE Transaction on Magnetics*, vol. 40, no. 1, pp. 85–96, Jan. 2004.
- [8] J. Rodriguez Arribas and C. Vega Gonzalez, "Optimal vector control of pumping and ventilation induction motor drives," *IEEE Transactions on Industrial Electronics*, vol. 49, no. 4, pp. 889 – 895, Aug. 2002.
- [9] S. Sangwongwanich, M. Ishida, S. Okuma, Y. Uchikawa, and K. Iwata, "Time-optimal single-step velocity response control scheme for field-oriented induction machines considering saturation level," *IEEE Transactions on Power Electronics*, vol. 6, no. 1, pp. 108–117, Jan. 1991.
- [10] M. A. Sheta, V. Agarwal, and P. S. V. Nataraj, "A new energy optimal control scheme for a separately excited dc motor based incremental motion drive," *International Journal of Automation and Computing*, vol. 6, no. 3, pp. 267–276, 2009.
- [11] G. Toacse and W. Culp, "Time-optimal control of a stepping motor," *IEEE Transactions on Industrial Electronics and Control Instrumentation*, vol. IECI-23, no. 3, pp. 291–295, Aug. 1976.
- [12] A. Trzynadlowski, "Energy optimization of a certain class of incremental motion dc drives," *IEEE Transactions on Industrial Electronics*, vol. 35, no. 1, pp. 60–66, Feb. 1988.
- [13] D. Zhang and G. Guo, "Discrete-time sliding mode proximate time optimal seek control of hard disk drives," *IEEE Proceedings- Control Theory and Applications*, vol. 147, no. 4, pp. 440–446, Jul. 2000.

Algorithm 2 The Main Algorithm for Computing Acceleration and Speed Constrained Energy-Optimal Trajectory

- 1: $i \leftarrow 1$, $\delta_i \leftarrow 0$, $\eta_i \leftarrow 1$, and choose $0 < \varepsilon \ll 1$
- 2: **while** $|\eta_i| > \varepsilon$ **do**
- 3: apply Algorithm 1 on interval $[0, t_f - \delta_i]$ with boundary conditions $v(0) = 0$, $x(0) = 0$, $v(t_f - \delta_i) = 0$, $x(t_f - \delta_i) = x_f - v_{\max}\delta_i$. Denote the solution by (x_i, v_i, u_i) .
- 4: solve $\dot{v}_i(t_{s_i}) = 0$ for t_{s_i}
- 5: $\eta_i \leftarrow v(t_{s_i}) - v_{\max}$
- 6: **if** $i=1$ **then**
- 7: **if** $\eta_i \leq 0$ **then**
- 8: $\eta_i \leftarrow 0$
- 9: **else**
- 10: $\delta_L \leftarrow 0$, $\delta_U \leftarrow \Delta_w = \frac{x_f}{v_{\max}} + \frac{v_{\max}}{2A_{\min}} - \frac{v_{\max}}{2A_{\max}}$
- 11: $\delta_{i+1} \leftarrow \frac{1}{2}(\delta_L + \delta_U)$
- 12: **end if**
- 13: **else**
- 14: **if** $\eta_i < 0$ **then**
- 15: $\delta_U \leftarrow \delta_i$
- 16: **else**
- 17: $\delta_L \leftarrow \delta_i$
- 18: **end if**
- 19: $\delta_{i+1} \leftarrow \delta_i - \left(\frac{\eta_i - \eta_{i-1}}{\delta_i - \delta_{i-1}}\right)^{-1} \eta_i$
- 20: **if** $\delta_{i+1} > \delta_U$ **or** $\delta_{i+1} < \delta_L$ **then**
- 21: $\delta_{i+1} = \frac{1}{2}(\delta_L + \delta_U)$
- 22: **end if**
- 23: **end if**
- 24: $i \leftarrow i + 1$
- 25: **end while**
- 26: $t_s \leftarrow t_{s_{i-1}}$, $\Delta_t^* \leftarrow \delta_i$, $(\tilde{x}^*, \tilde{v}^*, \tilde{u}^*) \leftarrow (x, v, u)$
- 27: **return** x^*, v^*, u^* , where

$$x^*(t) = \begin{cases} \tilde{x}^*(t), & 0 \leq t \leq t_s, \\ \tilde{x}^*(t_s) + v_{\max}(t - t_s), & t_s < t \leq t_s + \Delta_t^*, \\ \tilde{x}^*(t - \Delta_t^*) + v_{\max}\Delta_t^*, & t_s + \Delta_t^* < t \leq t_f, \end{cases}$$

$$v^*(t) = \begin{cases} \tilde{v}^*(t), & 0 \leq t \leq t_s, \\ v_{\max}, & t_s < t \leq t_s + \Delta_t^*, \\ \tilde{v}^*(t - \Delta_t^*), & t_s + \Delta_t^* < t \leq t_f, \end{cases}$$

$$u^*(t) = \begin{cases} \tilde{u}^*(t), & 0 \leq t \leq t_s, \\ (dv_{\max} + c)/b, & t_s < t \leq t_s + \Delta_t^*, \\ \tilde{u}^*(t - \Delta_t^*), & t_s + \Delta_t^* < t \leq t_f. \end{cases}$$